Magnetic characterization of Pr_2BaCuO_5

2008 J. Phys.: Condens. Matter 20 045210

(http://iopscience.iop.org/0953-8984/20/4/045210)

J. Phys.: Condens. Matter **20** (2008) 045210 (7pp) doi:10.1088/0953-8984/20/04/045210

Magnetic characterization of Pr_2BaCuO_5

R Sáez Puche[1], E Climent-Pascual[1], J Romero de Paz[1], M T Fernández-Díaz[2] and C Cascales[3]

[1] Departamento de Química Inorgánica I, Facultad de Ciencias Químicas, Universidad Complutense de Madrid, 28040 Madrid, Spain
[2] Institut Laue-Langevin, BP 156X, F-38042 Grenoble Cedex, France
[3] Instituto de Ciencia de Materiales de Madrid, CSIC, Cantoblanco, 28094-Madrid, Spain

E-mail: rsp92@quim.um.es, ecliment@quim.ucm.es, jromero@quim.ucm.es, ferndiaz@ill.fr and ccascales@icmm.csic.es

Received 3 October 2007, in final form 15 November 2007
Published 8 January 2008
Online at stacks.iop.org/JPhysCM/20/045210

Abstract

The magnetic behaviour of Pr_2BaCuO_5 oxide has been studied by means of magnetic susceptibility, magnetization, specific heat and neutron powder diffraction at low temperatures. This oxide behaves as an antiferromagnetic with a Néel temperature of 13.7 K and the magnetic structure can be described on the basis of a wavevector $\mathbf{k} = [0, 0, 0]$. The Cu^{2+} magnetic moments are aligned along the c-axis of the crystal structure, while the Pr^{3+} magnetic moments lie in the ab-plane with a small component along the c-axis. The experimental values of the ordered moments at 2 K are 0.9(3) and 0.8(3) μ_B for copper and praseodymium ions, respectively. The obtained set of crystal field parameters reproduces the paramagnetic susceptibility measurements and justifies the low experimental ordered moment of the Pr^{3+} ion.

(Some figures in this article are in colour only in the electronic version)

1. Introduction

R_2BaCuO_5 oxides constitute a subgroup of the large family of R_2BaMO_5 compounds, where R is a rare earth and M = Co, Ni, Cu and Zn [1]. These oxides, which crystallize with four different structural types, are the ideal scenario for testing the close relationships between structure and magnetic properties. Chemical substitution of either the transition metal M^{2+} or the R^{3+} cation will affect drastically the bulk magnetic properties of these compounds and their magnetic structures [2].

Most of the R_2BaCuO_5 oxides (for R being Sm, Lu and Y), crystallize with orthorhombic symmetry, space group $Pnma$ [3]; while the remaining oxides (for R being La, Pr and Nd), crystallize with the so-called Nd_2BaPtO_5 structural type showing tetragonal symmetry, space group $P4/mbm$ [4]. This latter structure shows as its main characteristic the presence of bi-capped trigonal $[RO_8]$ prisms sharing faces to form R_2O_5 layers that run perpendicular to the c-axis of the structure, as can be observed in figure 1. Between these layers are located square CuO_4 units, which are isolated from each other and connect the mentioned R_2O_5 layers. The larger barium atoms are coordinated by ten oxygen atoms forming bi-capped tetragonal prisms $[BaO_{10}]$.

Although many papers have been reported concerning the study of the optical and magnetic properties as well as the potential applications of the $Pnma$-R_2BaCuO_5 oxides ([5–7] and references therein), knowledge about the $P4/mbm$-R_2BaCuO_5 oxides is very scarce. It has been reported

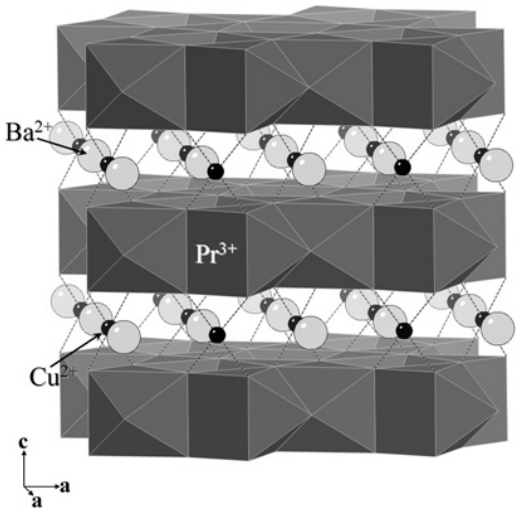

Figure 1. Perspective view of Nd_2BaPtO_5-type structure of the Pr_2BaCuO_5 oxide showing the $[RO_8]$ layers (grey polyhedra) and the square-planar $[CuO_4]$ polyhedra (sticks and balls).

that La_2BaCuO_5 oxide behaves as a ferromagnetic with a Curie temperature of 5.7 K [8] and their electronic structure has been explained by Eyert *et al* [9] using the standard spin polarized local density approximation, obtaining a ferromagnetic configuration for the ground state. The magnetic ordering is the origin of the splitting of the bands at the Fermi energy, opening a gap of about 0.35 eV and transforming the system into an insulator. Feldkemper *et al* [10] taking into account the crystal structure showed the existence of two main superexchange pathways through which the magnetic interactions take place. The predominant one involves the overlapping between the half-filled $d_{x^2-y^2}$ and the filled d_{z^2} orbitals of the nearest neighbour Cu^{2+} atoms located in the *ab* plane of the structure and, according to the Goodenough–Kanamori–Anderson (GKA) rules, the interaction should be ferromagnetic. However, the role of the rare earth elements in these isostructural compounds has remained puzzling, as the Nd_2BaCuO_5 oxide shows antiferromagnetic behaviour with a Néel temperature (T_N) of 7.5 K [11–14]; other studies revealed that the $LaEuBaCuO_5$ oxide remains ferromagnetic [15]. In this sense, more recently Nozaki *et al* [16] have reported a systematic study concerning the effect of the lanthanum substitution by other paramagnetic lanthanide cations on the ferromagnetism of the La_2BaCuO_5 oxide.

Bearing in mind this previous work, there are some important questions to be answered about the magnetic properties concerning this family of $P4/mbm$-R_2BaCuO_5 oxides such as: why does the sign of the magnetic interactions change dramatically from one compound to another and why are the magnetic structures so different for these compounds? To solve these questions we have undertaken a through study of the magnetic properties and magnetic structure of Pr_2BaCuO_5 oxide using different complementary physical measurements such as magnetization, magnetic susceptibility, specific heat and neutron diffraction at different temperatures.

2. Experimental details

Pr_2BaCuO_5 oxide was prepared by using a specific precursor method. Stoichiometric amounts of the precursor Pr_2CuO_4 oxide and $BaCO_3$ were heated at 950 °C for 12 h under flowing argon to stabilize the Pr^{3+} ion that is the oxidation state present in this compound. The obtained Pr_2BaCuO_5 oxide was dark brown in colour, and longer periods of reaction time or higher reaction temperatures give rise to the decomposition of the compound to $BaPrO_3$ oxide, which crystallizes with a distorted perovskite structure [17]. The precursor Pr_2CuO_4 oxide was obtained by firing stoichiometric amounts of Pr_6O_{11} (99.999%) and CuO (99.99%) in air at 1030 °C.

A temperature dependent neutron powder diffraction experiment was performed using the high-flux D20 diffractometer ($\lambda = 2.41$ Å) of the Institut Laue-Langevin (Grenoble, France). Several diffraction patterns were measured between 2 and 150 K over an angular range of 0°–150° in 2θ. The analysis of the diffraction data was based on the Rietveld method using the FullProf program [18].

Magnetization and magnetic susceptibility measurements were performed using a Quantum Design XL-SQUID magnetometer in the temperature range 2–300 K in different magnetic fields up to 5 T. Magnetic susceptibility measurements were carried out in zero field cooled (ZFC) and field cooled (FC) conditions. For ZFC measurements the sample was cooled from room temperature down to 2 K in the absence of a magnetic field. After applying a magnetic field at 2 K the susceptibility was measured in a warming cycle under the applied field. On the other hand, in the FC regime the sample was cooled in the presence of a magnetic field and then the susceptibility was measured by increasing the temperature from 2 to 300 K.

The specific heat measurements were performed in a Quantum Design PPMS in the temperature range 2–300 K by the heat phase-relaxation method using different magnetic fields up to 9 T. The powder sample was attached to a sapphire platform by a small amount of Apiezon N grease. The addenda heat capacity was measured in a separated run and subtracted for the sample data measurements.

3. Results and discussion

3.1. Structural characterization

X-ray diffraction data confirm the Nd_2BaPtO_5 type structure of the obtained Pr_2BaCuO_5 oxide as well as the presence of a small amount of the Pr_2CuO_4 precursor oxide. This structural type is characterized by the tetragonal space group $P4/mbm$. The barium, copper and one of the oxygen ions are occupying special positions, namely 2a (0, 0, 0), 2d (0, 1/2, 0) and 2b (0, 0, 1/2), respectively; while the other oxygen and praseodymium ions are located in 8k (x, y, z) and 4h (x, y, 1/2) general positions [19]. Structural parameters of the Pr_2BaCuO_5 oxide obtained from x-ray diffraction data have been used as initial values for the refinement of neutron diffraction data obtained at different temperatures between 150 and 2 K. Figure 2 shows the refined neutron diffraction pattern of Pr_2BaCuO_5 oxide obtained at 2 K. The small amount of the Pr_2CuO_4 precursor, around 4.4(2)%, was also included in the Rietveld refinement and its allowed Bragg reflections are noted in the second row of vertical marks on figure 2. The tetragonal symmetry remains for this oxide from room temperature down to 2 K.

Tables 1 and 2 collect the experimental values for the structural parameters obtained at 50 and 2 K. The slight decrease observed in the lattice parameters in going from 50 to 2 K is a consequence of the thermal contraction. Moreover, the oxygen atomic coordinates refined from these neutron diffraction data present a higher accuracy than those derived from the preliminary x-ray diffraction experiments [19]. The main bond distances and angles are also given in table 1. It can be observed that the square-planar units CuO_4 show four identical Cu–O distances but two different O–Cu–O planar angles, which it is indicative of a distortion away from the ideal D_{4h} symmetry.

It is worth noting that the intralayer Cu–Cu distance is 4.7270(1) Å, while the interlayer is larger taking a value of 5.8014(2) Å. The Cu–O–Pr bond angle is 174.14(9)°, which will have an important influence on the possible superexchange

Table 1. Rietveld refined lattice parameters, agreement factors, atomic positions, selected distances and angles for Pr_2BaCuO_5 at 50 K.

Formula		Pr_2BaCuO_5			
Crystal system		Tetragonal			
Space group		$P4/mbm$			
Cell parameters (Å)	a, c	6.6848(2)	5.8017(2)		
Volume (Å^3)		259.256(15)			
Rietveld R-factors	R_p	0.0985			
	R_{wp}	0.0959			
	χ^2	1.97			
Bragg R-factors	R_B	0.0198			
	R_f	0.0230			
Atom	Wyck.	Occ.	x/a	y/b	z/c
Pr	4h	1.00	0.1732(4)	0.6733(4)	1/2
Ba	2a	1.00	0	0	0
Cu	2d	1.00	0	1/2	0
O1	2b	1.00	0	0	1/2
O2	8k	1.00	0.3595(2)	0.8595(2)	0.7596(4)
β_{ov} (Å^2)	0.07(6)				
d(Cu–O) (Å)	O–Cu–O (deg)	d(Pr–O) (Å)	O–Pr–O (deg)		Cu–O–Pr (deg)
1.926(2) × 4	87.20(7) × 2	2.472(3) × 2	145.87(12) × 1	149.08(5) × 4	174.14(9) × 1
	92.80(7) × 2	2.317(3) × 2	81.09(5) × 1	61.67(8) × 2	93.86(7) × 2
	180.00(0) × 2	2.591(3) × 4	77.12(3) × 4	71.07(4) × 2	
			95.89(8) × 4	101.60(5) × 2	

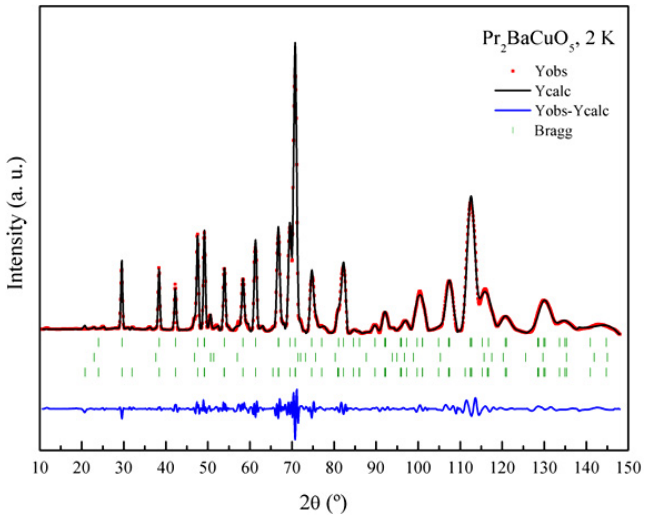

Figure 2. Rietveld refinement of the neutron diffraction pattern obtained at 2 K for Pr_2BaCuO_5 oxide. Vertical marks indicate the position of the allowed Bragg reflections for Pr_2BaCuO_5 (first row) and for the Pr_2CuO_4 precursor oxide (second row) which appears as impurity (4.4(2)%). The third row of vertical marks indicates the magnetic Bragg reflections for the proposed magnetic structure.

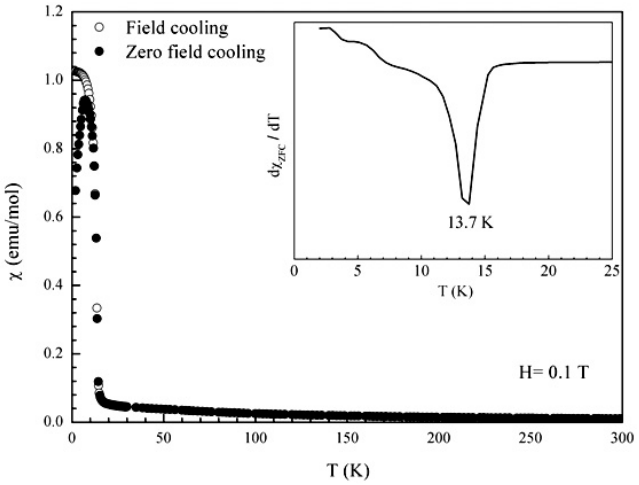

Figure 3. Temperature dependence of the FC and ZFC magnetic susceptibility. The inset shows the $d\chi/dT$ versus T plot.

magnetic interactions that will be the responsible for the magnetic interaction that will take place in this compound.

3.2. Magnetic behaviour

The temperature dependence of the FC and ZFC magnetic susceptibility for Pr_2BaCuO_5 oxide from 2 to 300 K in the presence of an applied magnetic field of 100 mT is depicted in figure 3. It has been determined that the magnetic susceptibility obeys the Curie–Weiss law from room temperature down to 25 K. The Weiss constant (θ) takes a value of −34 K and the obtained effective magnetic moment of 5.24 μ_B agrees well with the calculated 5.32 μ_B taking into account the Pr^{3+} and Cu^{2+} paramagnetic contributions. The negative value of θ is indicative of the onset of negative exchange correlations given as result 3D antiferromagnetic interactions between the magnetic moments. However, the magnetic susceptibility presents a sudden increase around 15 K that reveals the occurrence of a ferromagnetic component, which is fully confirmed from the noticeable difference found in the experimental values of the FC and ZFC magnetic susceptibility measurements below 15 K (see figure 3).

Table 2. Rietveld refined magnetic moments and agreement factors for Pr_2BaCuO_5 at 2 K.

Crystal structure				
Cell parameters (Å)	a, c	6.6843(2)	5.8006(2)	
Volume (Å^3)		259.172(16)		
Rietveld R-factors	R_p	0.0912		
	R_{wp}	0.0916		
	χ^2	2.76		
Bragg R-factors	R_B	0.0163		
	R_f	0.0090		
Magnetic structure				
Magnetic R-factor	0.0736			
	m_x (μ_B)	m_y (μ_B)	m_z (μ_B)	M (μ_B)
Pr^{3+}	0.18(6)	0.7(2)	0.27(10)	0.8(3)
Cu^{2+}	—	—	0.9(3)	0.9(3)

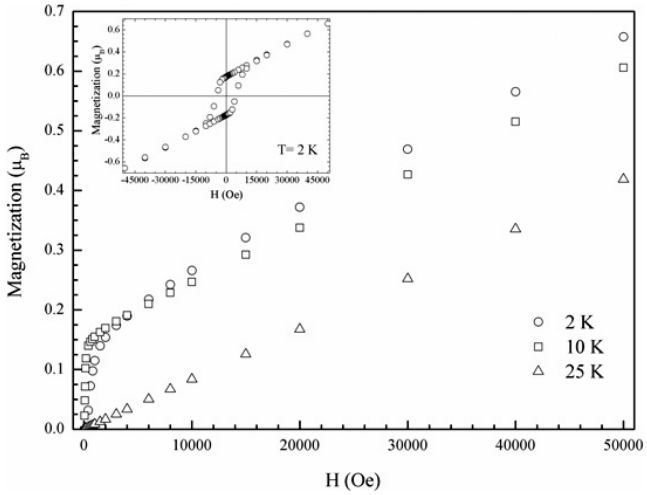

Figure 4. The magnetization against the magnetic field at different temperatures. The inset shows the hysteresis loop obtained at 2 K.

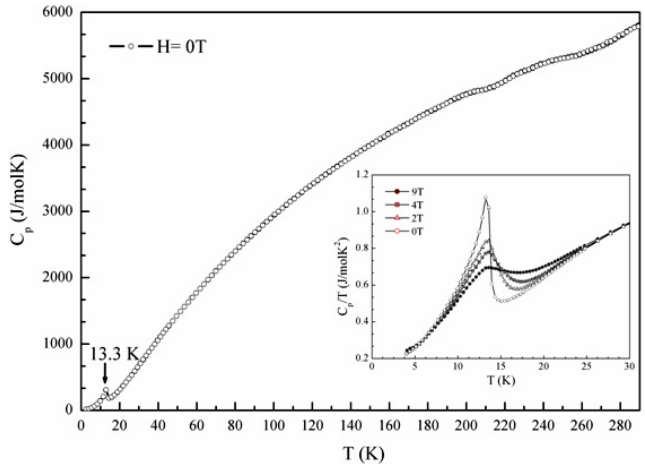

Figure 5. Temperature dependence of the magnetic specific heat. The inset represents the thermal variation of the specific heat at different magnetic fields.

The cooling of the sample under a magnetic field will favour the growth of the domains in the direction of the applied field and hence will result in a higher value of the magnetic susceptibility compared to the ZFC susceptibility. A magnetic ordering temperature $T_N = 13.7$ K, as indicated in the inset of figure 3, was assigned from the minimum of $d\chi/dT$ versus T curve, which corresponds to the steepest part of the susceptibility with decreasing temperature.

Afterwards the magnetization was measured as a function of the external field at different temperatures, as shown in figure 4. It can be observed that it follows a lineal behaviour above 0.4 T which is the typical feature for an antiferromagnetic material without any metamagnetic transition up to 5 T. The downwards deviations from linearity below 0.4 T can be attributed to the onset of the mentioned ferromagnetic component arising from the spin canting of antiferromagnetic ordered Pr^{3+} and Cu^{2+} sublattices. Moreover, as can be observed in the inset to figure 4, the hysteresis is removed above 2 T and the ferromagnetic component is as low as 0.17 μ_B, showing a coercive field of around 0.5 T. This weak ferromagnetic component is due to the antisymmetric Dzialoshinski–Moriya exchange involved in the Cu–O–Pr (174.14(9)°) pathway [20, 21].

All these data can be understood by considering a spin canting of the antiferromagnetically ordered Pr^{3+} and Cu^{2+} magnetic moments. On the other hand, the variation of the specific heat for this oxide between 2 and 300 K at different magnetic fields has been measured in order to study in depth the magnetic transition determined by the magnetic susceptibility measurements. As can be clearly observed in figure 5, the magnetic contribution to the specific heat, obtained after having subtracted both the lattice and electronic contributions [22], shows a λ-transition at 13.3 K, which corresponds to the Néel temperature previously determined from magnetic susceptibility measurements. The application of an external magnetic field influences the λ-transition significantly and it almost disappears at 9 T following the typical perturbation of an ordered magnetic state.

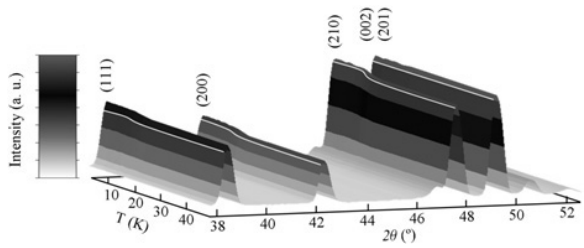

Figure 6. Thermal evolution of the neutron diffraction patterns in the temperature range 2–50 K.

3.3. Magnetic structure determination

The determination of the magnetic structure has been made from the analysis of the neutron diffraction patterns obtained from 150 to 2 K. Neutron diffraction patterns obtained at 150 and 50 K are almost coincident, but the neutron diffraction pattern obtained at 2 K shows the onset of very weak new reflections that can be ascribed to the presence of long-range magnetic ordering. All the magnetic reflections are denoted by the third row of vertical marks in figure 2. Furthermore, a detailed analysis of the thermal neutron diffraction patterns obtained in the temperature range 50–2 K reveals below 15 K an increase in the intensity of some nuclear Bragg reflections according to the temperature decrease, as can be observed in figure 6. These facts can be ascribed to the occurrence of long-range magnetic ordering, in such a way that all those magnetic reflections can be indexed successfully considering a propagation vector $\mathbf{k} = [0, 0, 0]$. Since both Pr^{3+} and Cu^{2+} sublattices become ordered at the same temperature, the basis vectors which describe the magnetic structure must belong to the same irreducible representation. Thus, the best agreement between the experimental and calculated neutron diffraction patterns has been reached considering the antiferromagnetic Pr^{3+} magnetic moments (m_{Pr}) coupled in the *ab*-plane of the structure with a small component along the *c*-axis, and the Cu^{2+} magnetic moments (m_{Cu}) antiferromagnetic aligned along the *c*-axis of the structure, as depicted in figure 7. It is worth noting that this non-collinear antiferromagnetic structure does not change from 2 to 15 K. A similar magnetic structure has been reported for Nd_2BaCuO_5 oxide [23], but a propagation vector $\mathbf{k} = [0, 0, 1/2]$ has been used to index the magnetic contribution to the diffraction patterns. The differences found in the magnetic structures could be attributed to the different anisotropy of the Pr^{3+} and Nd^{3+} ions.

A detailed mechanism through the magnetic interactions that take place in these $P4/mbm$-R_2BaCuO_5 oxides has already been given [15, 23] and it was established that the magnetic ordering is mainly governed by the effective orbital overlap of Cu–O–R superexchange interactions, where the half-filled $d_{x^2-y^2}$ orbital of Cu^{2+} is involved. This proposed pathway justifies the change of the sign of interactions from ferromagnetism in the La_2BaCuO_5 oxide to antiferromagnetism in the isostructural Pr_2BaCuO_5 and Nd_2BaCuO_5 oxides, where both Cu^{2+} and R^{3+} paramagnetic sublattices are involved in the superexchange interactions.

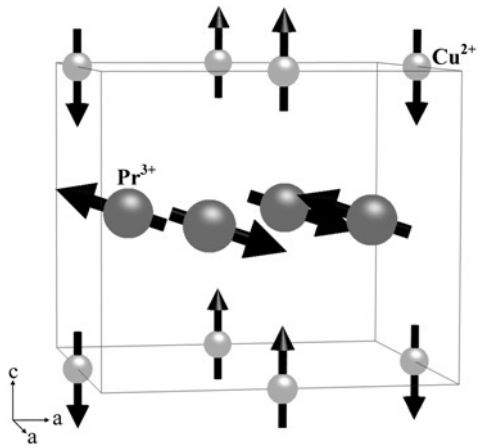

Figure 7. Magnetic structure for Pr_2BaCuO_5 oxide at 2 K, outlined within the crystallographic unit cell.

3.4. Magnetic susceptibility simulation from crystal field formalism

At 2 K, the lowest measuring temperature, the ordered magnetic moment of the Cu^{2+} ions takes a value of 0.9(3) μ_B (see table 2), which agrees well with the expected value $2S = 1$ μ_B, and the small difference between them may be assigned to covalency effects associated with the Cu–O bonds. However, in the case of the praseodymium ions the experimental ordered magnetic moment of 0.8(3) μ_B (see table 2) is significantly smaller than the expected ordered magnetic moment for the $^3H_4$ ground term of the free ion, $g_J \times J = 3.20$ μ_B [24].

To explain this rather low ordered magnetic moment of Pr^{3+}, an attempt has been made to derive the sequence of $^3H_4$ energy levels of Pr^{3+} in Pr_2BaCuO_5. For this we can use the correlation provided by the Van Vleck formalism [24] between an adequate reproduction of the measured thermal variation of the paramagnetic susceptibility curve and the sequence of energy levels for the $4f^2$ electronic configuration of Pr^{3+} in Pr_2BaCuO_5. Only the contribution of Pr^{3+} should be considered in the experimental curve, which requires the removal of that one corresponding to Cu^{2+}. With the theoretical background developed previously for the crystal field (CF) interactions of the rare earth in this structure [11], different sequences of Pr^{3+} energy levels derived from sets of semi-empirical C_{2v} CF parameters, obtained using the simple overlap model (SOM) values [25] and then adapted with regards to the previous phenomenological CF analysis in isostructural Nd_2BaCuO_5 [11], were tested in the calculation of the paramagnetic contribution of Pr^{3+} in the thermal evolution of χ_m in Pr_2BaCuO_5, and also in the evolution of its magnetic moment.

Figure 8 gives the best fit between measured and simulated $Pr^{3+}\chi_m^{-1}$ curves. The experimental data have been fitted down to 35 K because at lower temperatures the paramagnetic state is perturbed due to the onset of the mentioned antiferromagnetic interactions. Table 3 includes the corresponding set of free ion and CF parameters, which yields the sequence 0, 100, 204, 236, 254, 469, 590, 753 and 841 cm^{-1} as CF

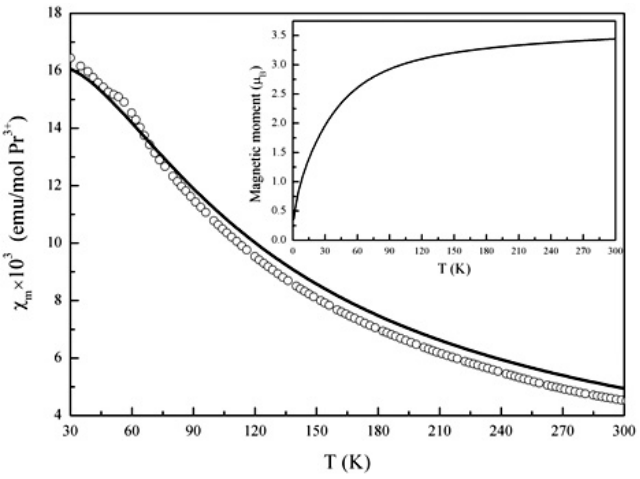

Figure 8. Comparison between experimental (circles) and simulated (from crystal field parameters, line) curves of the thermal evolution for the inverse of the paramagnetic susceptibility per mol of Pr^{3+} in Pr_2BaCuO_5. The inset shows the variation of the magnetic moment from CF effects on Pr^{3+}.

Table 3. Free ion [26, 27] FI and crystal field CF parameters (cm^{-1}) for Pr^{3+} used in the calculation of the paramagnetic contribution of Pr^{3+} in the thermal evolution of χ_m in the Pr_2BaCuO_5.

FI		CF	
E^0	9548.58	B_0^2	−580
E^1	4563	B_2^2	220
E^2	22.82	B_0^4	−1550
E^3	474.80	B_2^4	−1775
α	19.84	B_4^4	400
β	−705	B_0^6	650
γ	1400	B_2^6	320
ζ	685	B_4^6	425
$M^{0\,a}$	1.40	B_6^6	−410
$P^{2\,b}$	50		

[a] M^0, M^2, M^4 were constrained by the ratios $M^2 = 0.56M^0$, $M^4 = 0.32M^0$.
[b] P^2, P^4, P^6 were constrained by the ratios $P^4 = 0.75P^2$, $P^6 = 0.50P^2$.

energy levels for $^3H_4$. The deviation observed between experimental and calculated curves is due to some uncertainty in current CF parameters; however, given the similarity of these latter with the phenomenological ones for the isostructural Nd_2BaCuO_5 [11], the obtained sequence of $^3H_4$ energy levels and their associated wavefunctions can be considered realistic. The value of 0.8(3) μ_B obtained for ordered Pr^{3+} ions can thus be explained by taking into account that the first excited energy level $^3H_4(1)$ is situated at 100 cm^{-1} above $^3H_4(0)$, and thus at 2 K the contribution to the magnetic moment comes from the only populated ground level. The inset to figure 8 shows the evolution with temperature of the Pr^{3+} magnetic moment as calculated from the above determined $4f^2$ wavefunctions. It can be seen that the model predicts magnetic moments of ∼0.8 μ_B for temperatures below 6 K.

4. Conclusions

The crystal structure of the oxide Pr_2BaCuO_5 has been studied from neutron diffraction data obtained in the temperature range 50–2 K, showing tetragonal symmetry, space group $P4/mbm$, in the whole temperature range. Bulk magnetic measurements reveal the presence of antiferromagnetic ordering at T_N = 13.7 K, with the onset of a weak ferromagnetic component. The change of the sign of interactions compared with the ferromagnetic La_2BaCuO_5 oxide could be due to the presence of paramagnetic Pr^{3+} giving rise to the predominant Cu–O–Pr superexchange interactions, which yield a simultaneous ordering in the copper and praseodymium sublattices. The analysis of the neutron diffraction pattern obtained at 2 K has allowed us to determine the magnetic structure of the Pr_2BaCuO_5 oxide. The structure can be described with a propagation vector $\mathbf{k} = [0, 0, 0]$ and the ordered m_{Cu} are aligned along the c-axis, while the ordered m_{Pr} are mainly located in the basal plane of the structure. The onset of a weak ferromagnetic component which appears at the ordering temperature, negligible from these neutron diffraction data, is due to the spin canting arising from the antisymmetric Dzialoshinski–Moriya exchange. Crystal field simulation has been performed for the Pr^{3+} ion, obtaining a good agreement between the experimental and calculated magnetic susceptibilities, and it justifies the low experimental ordered magnetic moment of Pr^{3+}, 0.8(3) μ_B, compared with that one corresponding to the free ion ground state, $^3H_4$, which takes a value of 3.20 μ_B.

Acknowledgment

Thanks are due to Spanish MEC for financial support under research project MAT2006-13459-C01-02.

References

[1] Sáez Puche R and Hernández Velasco J 1994 *J. Adv. Mater. Res.* **1/2** 65
[2] Hernández Velasco J 2001 *PhD Thesis* Universidad Complutense Madrid
[3] Salinas A, García J L, Rodríguez-Carvajal J, Sáez Puche R and Martínez J L 1992 *J. Solid State Chem.* **100** 201
[4] Schiffler S and Müller-Buschbaum H K 1986 *Monatsch. Chem.* **117** 465
[5] Chattopodhgay T, Brown P J, Kobler U and Wihelm E 1989 *Europhys. Lett.* **8** 685
[6] Golosovsky I V, Plakhty V P, Hauchenhov V P, Zoulkova J, Mill B V, Bonnet M and Roudeau E 1992 *Sov. Phys.—Solid State* **34** 782
[7] Salinas Sánchez A, Sáez Puche R and Alario M A 1990 *J. Solid State Chem.* **89** 361
[8] Mizuno F, Masuda H, Hirabayashi I, Tanaka S, Hasegawa M and Mizutani U 1990 *Nature* **345** 788
[9] Eyert V, Hock K-H and Riseborough P S 1995 *Europhys. Lett.* **31** 385
[10] Feldkemper S, Weber W, Schulenburg J and Richter J 1995 *Phys. Rev.* B **52** 313

[11] Sáez Puche R, Climent E, Romero de Paz J, Martínez J L, Monge M A and Cascales C 2005 *Phys. Rev.* B **71** 024403
[12] Paukov I V, Popova M N and Mill B V 1991 *Phys. Lett.* A **157** 306
[13] Golosovsky I V, Boni P and Fischer P 1993 *Phys. Lett.* A **182** 161
[14] Goodenough J B 1976 *Magnetism and the Chemical Bond* (New York: Krieger)
[15] Salinas-Sánchez A and Sáez Puche R 1993 *Solid State Ion.* **63–65** 927
[16] Nozaki H, Ikuta H, Yamada Y, Matsushita A, Takahashi H, Hirabayashi I and Mizutani U 2000 *Phys. Rev.* B **62** 9555
[17] Jacobson A J, Tofield B C and Fender B E F 1972 *Acta Crystallogr.* B **28** 956
[18] Rodríguez-Carvajal J 1993 *Physica* B **192** 55
[19] Sáez-Puche R, Herrera S R and Martínez J L 1998 *J. Alloys Compounds* **269** 57
[20] Dzialoshinski I 1958 *J. Phys. Chem. Solids* **4** 241
[21] Moriya T 1960 *Phys. Rev.* **120** 91
[22] Gopal E S R 1966 *Specific Heats at Low Temperatures* (New York: Plenum)
[23] Sáez Puche R, Climent E, Jiménez-Melero E, Romero de Paz J, Martínez J L and Fernández-Díaz M T 2006 *J. Alloys Compounds* **408–412** 613
[24] Van Vleck J H 1932 *The Theory of the Electric and Magnetic Susceptibilities* (Oxford: Oxford University Press)
Van Vleck J H 1968 *J. Appl. Phys.* **39** 365
[25] Porcher P, Couto dos Santos M and Malta O 1999 *Phys. Chem. Chem. Phys.* **1** 397
[26] Cascales C, Sáez Puche R and Porcher P 1995 *J. Solid State Chem.* **114** 52
[27] Cascales C and Zaldo C 2006 *Chem. Mater.* **18** 3742